

PARTICLE PRODUCTION AT AGS ENERGIES *

S.G. STEADMAN, P.J. ROTHSCHILD, T.W. SUNG, and D. ZACHARY

Laboratory for Nuclear Science and Physics Department

Massachusetts Institute of Technology

Cambridge, MA 02139-4307, USA

for the E802 Collaboration

ABSTRACT

We discuss particle production from 14.6 A-GeV/c Si and 11.6 A-GeV/c Au projectiles on Al and Au targets. The second-level trigger utilized by E859 allows high precision measurements of K^- , \bar{p} , Λ and $\bar{\Lambda}$. The $\bar{\Lambda}$ yield is larger than expected, and a surprisingly large fraction of the \bar{p} 's are observed to arise from the decay of $\bar{\Lambda}$.

1. Introduction

At AGS energies of 11-15 A-GeV/c one achieves a high degree of stopping, thereby reaching the highest baryon densities achievable in heavy-ion reactions. Indeed, cascade Monte Carlo calculations, such as ARC¹, indicate that densities exceeding 9 times the ground state nuclear matter density may be achievable in Au+Au collisions. It is generally believed that densities exceeding 5-6 times normal density are required to make the transition to the quark-gluon plasma (QGP) phase. If such new physics is to be observed, it is important to provide a broad base of data for comparison to such Monte Carlo models in order to test their validity.

This work concentrates on the systematics of particle production from the series E802/E859/E866 of experiments at the Brookhaven AGS. The very successful implementation of the second level trigger in E859 with Si beams allows the E802 spectrometer to perform on-line particle identification within 40 μ s. This allows an event selectivity that increases the data taking rate by up to an order of magnitude, providing a far better data sample for the detection of particles such as K^- and \bar{p} .

2. Experiment

The E802 spectrometer² consists of a 25 msr acceptance rotatable single arm spectrometer that can be used together with event characterization devices to obtain semi-inclusive spectra and measure two-particle correlations. For asymmetric collisions, such as 14.6 GeV/c Si+Au, a target multiplicity array (TMA) sensitive to a large fraction of the total charged particles emanating from the target, is used to

*This research was supported by the U.S. Department of Energy, Division of Basic Energy Sciences under Contract No. DE-AC02-76CH00016.

select the collision geometry, specifically the upper 7% of the interaction cross-section (central collisions) or lower 50% (peripheral collisions). The central trigger corresponds roughly to a range of impact parameters for which the Si projectile is totally occluded by the Au target. For the symmetric Si+Al collisions at 14.6 GeV/c, as well as Au+Au collisions at 11.6 A·GeV/c incident momentum, a zero-degree calorimeter is used to measure the forward going energy in a cone of ≈ 1.5 degrees relative to the beam axis. By dividing this measured forward energy by the kinetic energy per projectile nucleon we obtain the mean number of projectile participants.

3. Pion production

Of particular interest is the determination of the number of produced pions per participant. At AGS energies the dominant part of the inelastic N-N cross section is excitation of the nucleon resonances Δ and N^* .¹ Indeed, ARC calculations³ indicate that a large fraction of the participants in central Au+Au collisions become these excited baryonic resonances. One might expect, then, that in the subsequent decay one would observe about one produced pion per participant. The charged pion distributions are observed to have an exponential dependence on p_{\perp} , with inverse slopes typically about 160 MeV/c at mid-rapidity. By integrating over p_{\perp} one obtains the rapidity distribution, for which our acceptance covers approximately 80% of the total yield. Assuming a Gaussian form for dN/dy , we show in Fig. 1 the phase space integrated π^+ multiplicity as a function of measured projectile participants, as determined by ZCAL for 11.6 A·GeV/c Au+Au collisions and 14.6 A·GeV/c Si+Al collisions. (One should note that the energy of the Au beam is somewhat lower than for the Si beam, which from p-p systematics would lead one to expect about a 14% reduction in the π^+ yield.) The obvious linear dependence is seen. From a similar observed dependence for π^- and assuming that the yield for π^0 is the mean of the π^+ and π^- yield, one obtains an overall multiplicity of 1.2 produced pions per participant.

4. Kaon and lambda production

We now turn to strangeness production, whose enhancement has long been considered a signal for QGP production⁴ and whose observation by E802⁵ and others has stimulated much theoretical interest. With the combined use of the second level trigger and extended particle ID using a segmented threshold gas Čerenkov detector, we have far more precise data available for both K^+ and K^- production. The invariant cross sections per trigger (TMA central or peripheral) are found to be well described by exponentials in the transverse mass, $m_{\perp} = \sqrt{p_{\perp}^2 + m^2}$. The fitted inverse slope parameters, as a function of rapidity, are shown in Fig. 2 for both central and peripheral Si+Al and Si+Au collisions. Unlike pion production, the inverse slope parameters depend on centrality and generally these more central collisions have higher inverse

DISCLAIMER

This report was prepared as an account of work sponsored by an agency of the United States Government. Neither the United States Government nor any agency thereof, nor any of their employees, make any warranty, express or implied, or assumes any legal liability or responsibility for the accuracy, completeness, or usefulness of any information, apparatus, product, or process disclosed, or represents that its use would not infringe privately owned rights. Reference herein to any specific commercial product, process, or service by trade name, trademark, manufacturer, or otherwise does not necessarily constitute or imply its endorsement, recommendation, or favoring by the United States Government or any agency thereof. The views and opinions of authors expressed herein do not necessarily state or reflect those of the United States Government or any agency thereof.

DISCLAIMER

Portions of this document may be illegible in electronic image products. Images are produced from the best available original document.

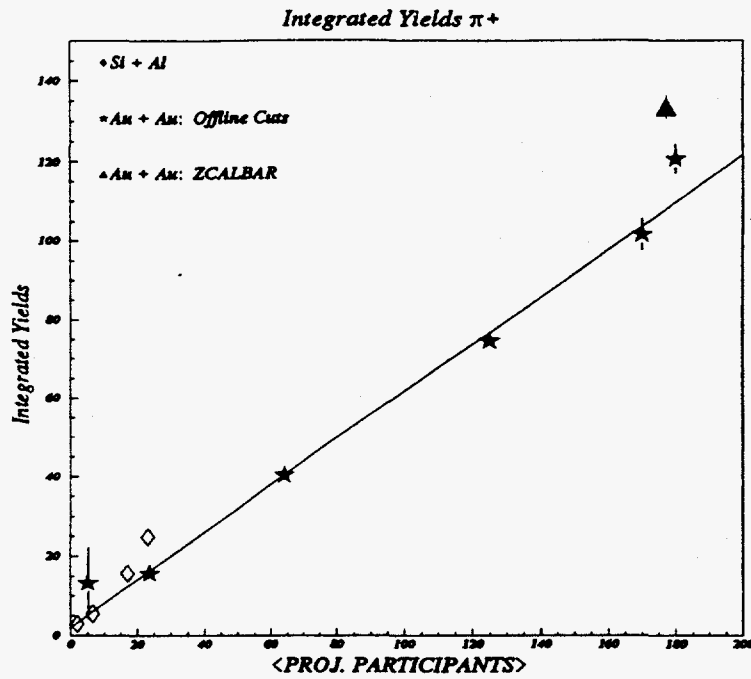


Fig. 1: Integrated yields of π^+ as a function of projectile participants for ^{28}Si and ^{197}Au projectiles.

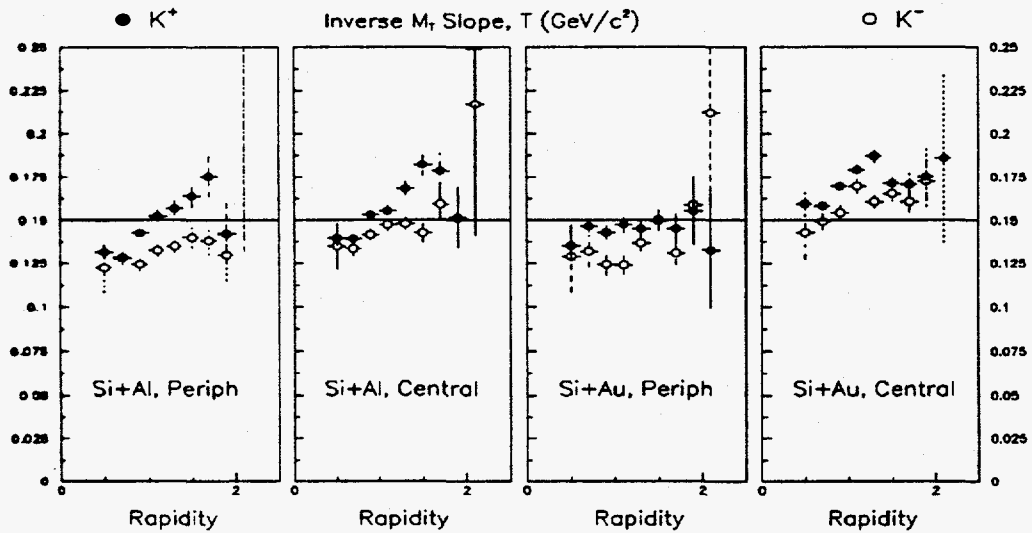


Fig. 2: E859 K^{\pm} inverse m_{\perp} slopes versus rapidity for peripheral and central Si+Al and Si+Au collisions.

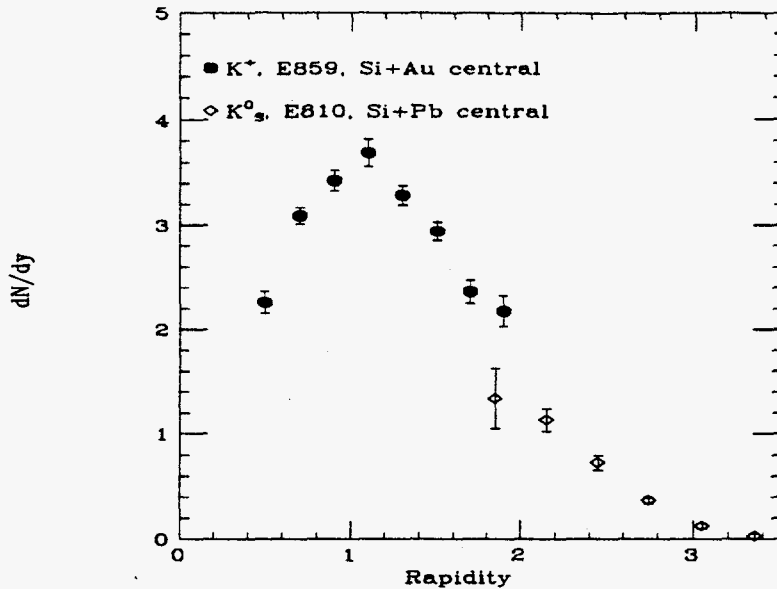


Fig. 3: E859 K^+ yield versus rapidity for central Si+Au collisions. The E810 K_S^0 yield versus rapidity is also shown for central Si+Pb collisions.

slope parameters at a given rapidity. The K^+ tend to have larger inverse slope parameters than K^- for a given target and centrality. These transverse mass distributions can be integrated to yield rapidity distributions, dN/dy . Fig. 3 shows our results for K^+ 's from central Si+Au collisions, together with other AGS measurements from E810 for K_S^0 production in central Si+Pb collisions (albeit with a somewhat different centrality trigger).⁶ It is noteworthy that the dN/dy for K^+ peaks at a rapidity of 1.1, behind the participant center-of-mass rapidity of 1.3 for central Si+Au collisions. Rescattering mechanisms, such as $\rho N \rightarrow K\Lambda$ have been suggested⁷ as likely mechanisms for producing the observed enhancement. Such secondary collisions have peak yields at a lower rapidity than the participant rapidity. Thus, the observed rapidity distribution may be consistent with this mechanism.

To provide a measure of how the different mechanisms contribute to K^+ production, we have also measured the Λ production at y about 1.4. This was done by observing the Λ decay products, (p, π^-) , for which the invariant mass distribution is shown in Fig. 4. Background distributions were obtained using (p, π^-) pairs with the protons and pions coming from different events. Invariant mass distributions for four p_\perp intervals were generated for central collisions (upper 20% of the TMA multiplicity distribution). Background subtraction was done for each interval to obtain the number of Λ 's for that interval. No vertex cuts were required on the Λ candidates. The large, momentum dependent acceptance correction was obtained by a Monte Carlo analysis. This was checked by using the acceptance to determine the Λ decay constant from the data. Our determined value for $c\tau = 7.98 \pm 0.65$ cm is in agreement with the accepted value⁸ of 7.89 cm, giving us confidence in the validity of this acceptance correction. From an exponential m_\perp fit to the four bins (Fig. 5), we obtain an inverse

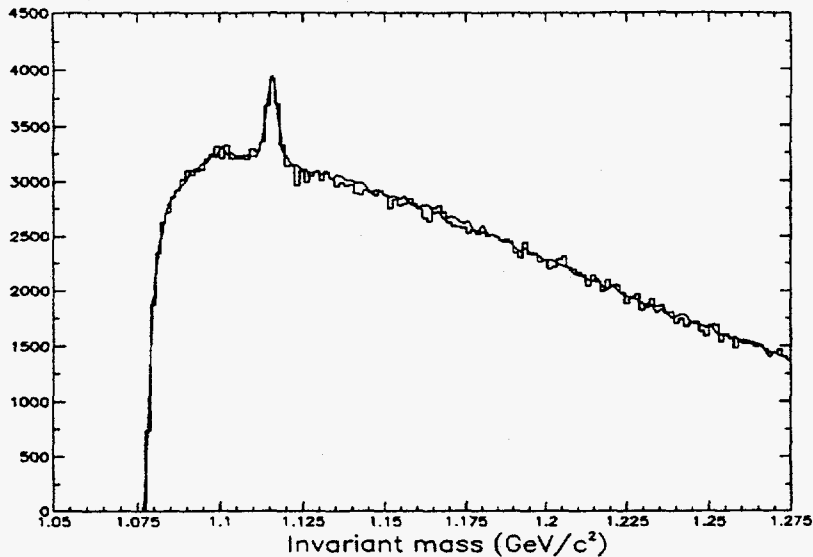


Fig. 4: The invariant mass distribution of (p, π^-) pairs from central Si+Au collisions.

slope parameter of $171 \pm 13 \text{ MeV}/c^2$. Integrating over m_{\perp} gives a rapidity density at this rapidity of 3.85 ± 0.58 . A surprising result is the K^+/K^- ratio, as shown in the left panel of Fig. 6, for both central and peripheral Si+Al and Si+Au collisions. The rapidity dependence of the ratio is found to be independent of target and centrality. A similar rapidity dependence is also found for Au+Au collisions (right panel) though the statistics are poorer.

5. Antiproton and antilambda production

Because of the large energy required to produce a \bar{p} in NN collisions at the AGS, one is very near threshold ($E_{\text{th}} = 4m_{\text{proton}} = 3.8\text{GeV}$, $E_{\text{cm}} = 5.4\text{GeV}$). Thus, one expects that the \bar{p} production is particularly sensitive to the earlier stage of the collision, and therefore to possible QGP production. The on-line second level triggering capability of E859 allowed an order of magnitude improvement in statistics compared with E802.⁹ Fig. 7 shows the extracted inverse m_{\perp} slopes for central and minimum bias Si+Al and Si+Au collisions. The new data are consistent with the earlier E802 data, but with much greater precision. Overall, these inverse slope parameters are lower than for protons, but are similar to those obtained for the protons for central Si+Au. This is somewhat surprising. One proposed explanation for the large proton inverse slope parameter is the increased boost in p_{\perp} given by multiple N-N collisions. The decay of these excited baryons yields an additional boost to the proton p_{\perp} . For \bar{p} , however, one does not expect significant rescattering, due to the high annihilation cross section. Thus, one would expect the mean p_{\perp} for the \bar{p} to be similar to the produced π 's and K 's, as observed in the minimum bias data.

Even though the cross-section for $\bar{\Lambda}$ production is very small, we have been able to measure the $\bar{\Lambda}/\Lambda$ ratio (integrated over the spectrometer acceptance) by switching

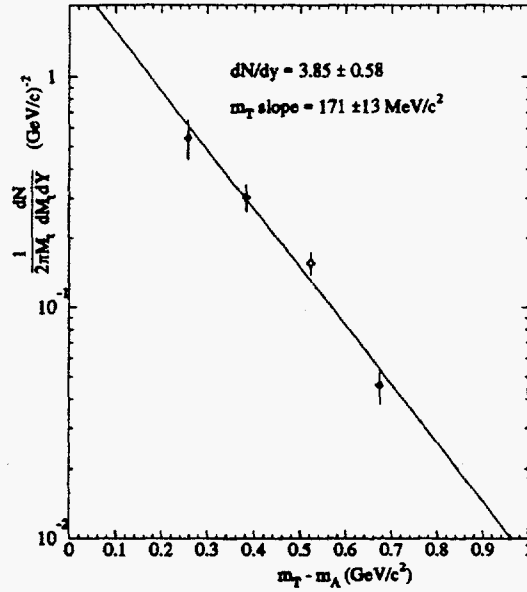


Fig. 5: E859 Λ m_{\perp} distribution for central Si+Au collisions.

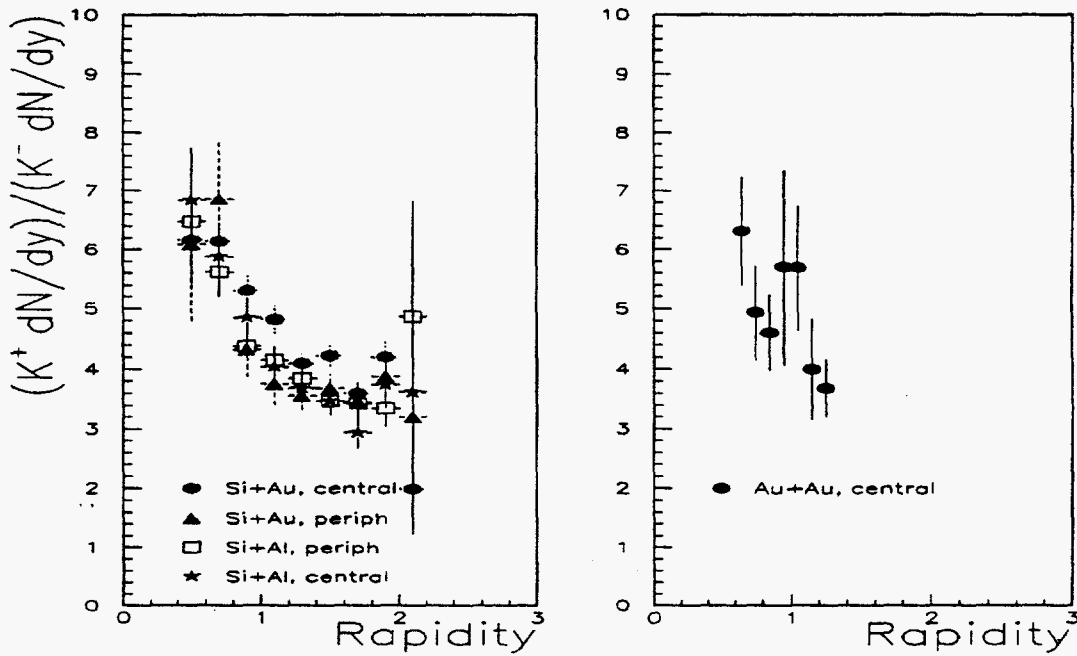


Fig. 6: E859 K^+/K^- ratio versus rapidity for central and peripheral Si+Al and Si+Au collisions (left panel). The right panel shows the same ratio for central Au+Au collisions.

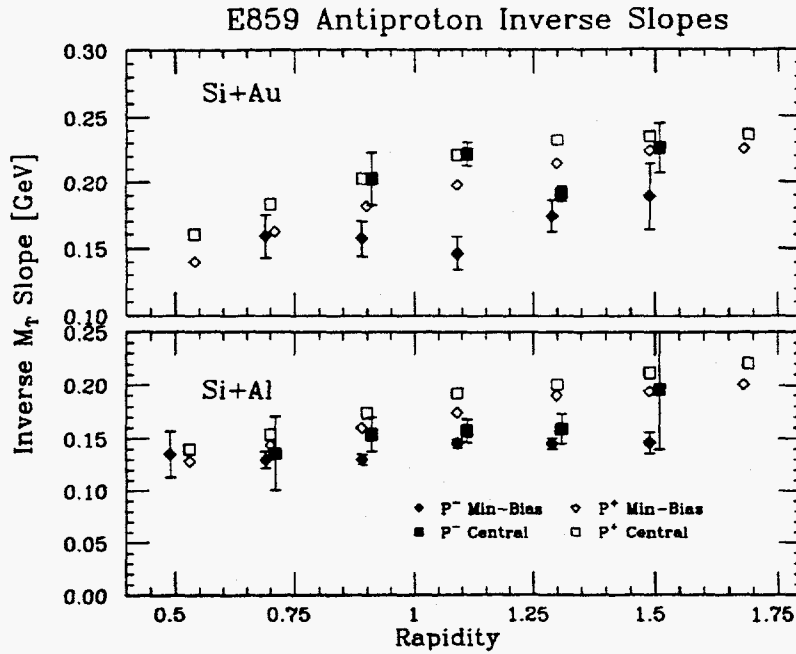


Fig. 7: Inverse m_{\perp} slope parameters for antiprotons in Si+Al and Si+Au collisions.

the direction of the spectrometer magnetic field at the same angle setting of the spectrometer for which the Λ measurement was made and recording the opposite charged particles (\bar{p} , π^+). The lower \bar{p} yield results in a much reduced combinatoric background. This is shown by the (\bar{p} , π^+) invariant mass distribution in Fig. 8. The only correction required in order to obtain the ratio is the simple correction for the \bar{p} 's that annihilate within the spectrometer ($\approx 5\%$). The spectrometer-integrated $\bar{\Lambda}/\Lambda$ ratio within the same rapidity interval about $y=1.4$ is $(3.7 \pm 0.5 \pm 0.3) \times 10^{-3}$, where the errors are statistical and systematic, respectively. With the correction for the decay branch to \bar{p} 's one obtains that $(63 \pm 13 \pm 11)\%$ of the \bar{p} 's within the rapidity interval would arise from $\bar{\Lambda}$ decay. It should be noted that this result depends on the assumption that the Λ and $\bar{\Lambda}$ have similar inverse slope parameters (similar slopes have been observed by NA36 for S+W at 200 A-GeV/c)¹⁰ and that the \bar{p} 's from the $\bar{\Lambda}$ decay have the same rapidity distribution as the $\bar{\Lambda}$'s (confirmed by a Monte Carlo study). This large value for $\bar{\Lambda}$ production could explain two striking features of the \bar{p} production, which otherwise are hard to understand, namely the large inverse slope parameters and the large yield for central Si+Au collisions. The latter may result from the relatively small annihilation cross section of $\bar{\Lambda}$'s compared with \bar{p} 's in the nuclear medium.

6. Conclusions

Even though calculations such as ARC predict high baryon densities, the volume of this high density region is small compared with the total interaction volume. Thus,

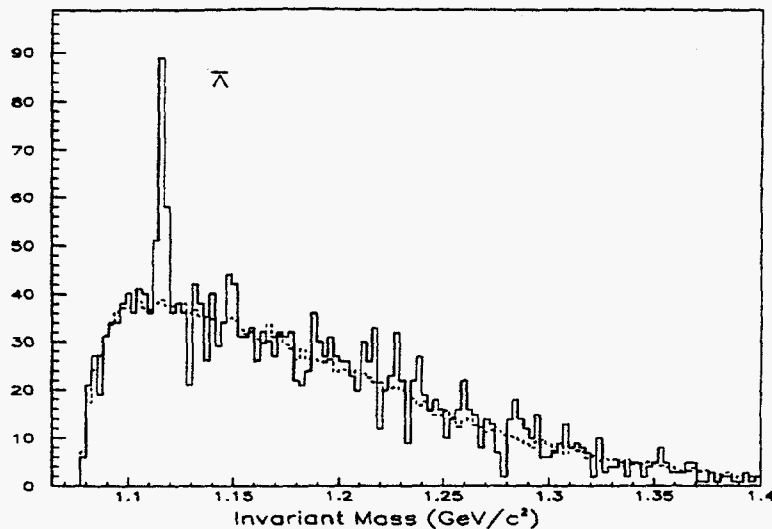


Fig. 8: Invariant mass spectrum of (\bar{p}, π^+) pairs from central Si+Au collisions. The scaled background is shown by the dashed curve. Both the \bar{p} and π^+ were required to be fully in the spectrometer acceptance.

it seems likely that any signal for QGP formation will be found in weak signals, such as strangeness production, and more likely in extremely rare processes such as $\bar{\Lambda}$ production. The preliminary indications from the data indicate that the $\bar{\Lambda}/\Lambda$ ratio is considerably larger than what one expects from a cascade code calculation.¹¹ Further measurement will be required to extend the rapidity range. More importantly, the recently commissioned Au beam offers the opportunity to create a much larger volume of high density nuclear matter. Under these conditions it will be particularly interesting to see if such large $\bar{\Lambda}$ yields are observed.

7. References

- [1] Y. Pang *et al.*, *Phys. Rev. Lett.* **68**, 18 (1992).
- [2] T. Abbott *et al.*, *Nucl. Inst. Meth. A* **290**, 41 (1990).
- [3] S. Kahana *et al.*, in *Heavy-Ion Physics at the AGS: HIPAGS'93*, edited by G.S.F. Stephans, S.G. Steadman, and W.L. Kehoe, MITLNS-2158 (1993), p.263.
- [4] P. Koch, B. Müller, and J. Rafelski, *Phys. Rep.* **142**, 167 (1986).
- [5] T. Abbott *et al.*, E802 collaboration, *Phys. Rev. Lett.* **64**, 847 (1990).
- [6] A.C. Saulys *et al.*, E810 collaboration, in *HIPAGS'93*, *op cit.*, p. 196.
- [7] H. Sorge, in *HIPAGS'93*, *op cit.*, p. 283.
- [8] *Review of Particle Properties*, *Phys. Lett. B* **239** (1990).
- [9] T. Abbott *et al.*, E802 collaboration, *Phys. Lett. B* **271**, 4477 (1991).
- [10] R. Zybent and E. Judd, *Particle Production in Highly Excited Matter*, edited by H.H Gutbrod and J. Rafelski, (Plenum Press, NY, 1993), p. 545.
- [11] A. Jahns, private communication